WAVE-WAVE INTERACTIONS, CURRENT-WAVE INTERACTIONS AND RESULTING EXTREME WAVES AND BREAKING WAVES

by

SØREN PETER KJELDSEN & DAG MYRHAUG
Senior Research Engineers

Norwegian Hydrodynamic Laboratories
Trondheim, Norway

ABSTRACT

The influence of an opposing current on highly non-linear transient breaking waves in deep water is described quantitatively from experiments. 3 new parameters that describe crest front steepness and wave asymmetry are introduced. Further, joint probability density distributions are obtained from an analysis of field data containing nearly 25000 storm waves. Thus, a tool is provided from which estimates for probabilities for occurrences of steep breaking waves in deep water, may be obtained.

1. INTRODUCTION

Detailed knowledge of the kinematics, dynamics and frequencies for occurrences of large breaking waves in deep water is important, and has many practical applications, due to the following reasons:

1) Experiments have now confirmed that transient, near breaking and breaking waves attain velocities up to 2.8 times the first order phase velocity. Local accelerations in the wave can attain values somewhat above 3 times the gravity acceleration (KJELDSEN et al., 1980). Such results may be applied to evaluation of the operation and stability of ships under severe sea conditions. Further,

such results provide the basis for the estimation of wave drag and inertia forces from extreme breaking waves in deep water with many applications to the design and safety of offshore structures.

2) The large breaking waves give rise to the largest environmental pressures, both on fixed and floating structures, in the form of shock or impact impulses with a duration of some milliseconds.

3) The breaking waves give rise to the most effective mechanism for transfer of momentum from the wind to a mean surface current, (dominant compared with dissipation of non-breaking waves, LONGUET-HIGGINS, 1969). This implies that a detailed knowledge of ratios of breaking waves compared to the total number of waves has important practical applications for the evaluation of dispersion of pollution (e.g. hydrocarbons).

In order to evaluate safety at sea, a basic need is a prediction of the characteristics of extreme sea states. There is an extensive literature on the subject of the mysterious disappearances of ships, both large and small. A high percentage of these mysteries can be solved by even a cursory study of so-called 'freak waves' (a freak being 'capricous change'), which are more correctly termed extreme waves. In the following the term extreme waves will be used, since these are recurring events along the continental margins. Extreme waves occur in virtually all such areas during certain predictable times of the year, but the origin of these waves is not fully understood. It is believed that a shoaling mechanism, unique to a certain geographic location, as well as particular random phase relationship between waves, can account for the phenomenon. However, also an opposing shear current might change the wave conditions in an abrupt way, in particular in areas where the waves travel against a current gradient. Known areas of destructive waves are the Nova Scotia coast, the Bermuda rise, the water off Greenland, the coast of North West India, and the water off the South East African coasts, where the Agulhas current opposes the main dispersion direction of the waves. Also certain parts of the Norwegian Continental Shelf seem to contain areas where such extreme waves occur. In the

period 1970-1979, 26 Norwegian trawlers and freighters were lost due to capsizing in very rough seas. Reports from the Courts of Inquiry show that for 13 of these vessels surviving members of the crew confirmed a capsizing in extreme waves. In 13 other cases the vessels disappeared in very bad weather, the reasons being unknown, but capsizings in extreme waves were concluded to be the most probable. Altogether 72 lives were lost. (NEDRELID, 1978.)

In 1978 a new project, "SHIPS IN ROUGH SEAS", was initiated by a coordinating board with the Royal Norwegian Council for Scientific and Industrial Research, the Norwegian Fisheries Research Council and the Norwegian Maritime Directorate as sponsors. The aim is to use theoretical and experimental work and practical experience to improve the understanding of manoeuvering, rolling and capsizing, i.e. the response of ships to severe conditions in the form of extreme movements. Further, it is the aim of the project to try to establish new criteria for the stability of the vessels on the basis of knowledge of extreme environmental conditions and the motion properties of the vessel. This will be an improvement compared to the established stability criteria which consider movement of a ship in calm water or in regular waves. One of the main activities for this new project is:

> *To locate exposed areas in Norwegian waters where the probabilities for occurrences of extreme waves and breaking waves are most pronounced, and contribute to the development of forecast methods for such areas.*

Results of a survey of areas on the Norwegian Continental Shelf with typical large scale refraction and current-wave interaction effects are shown in Fig. 1 (KJELDSEN & MYRHAUG, 1978). Also, positions and estimated headings are shown for 24 of the lost vessels.

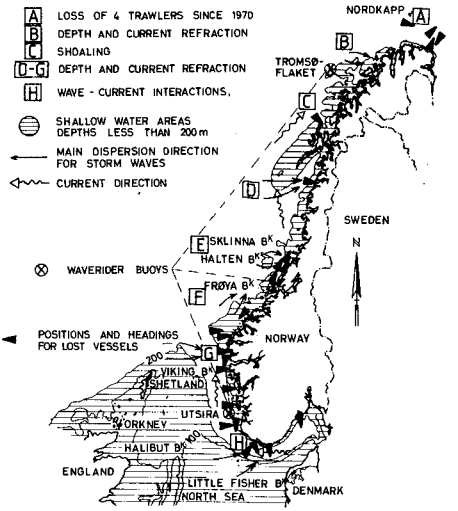

Fig. 1. *Exposed areas on the Norwegian Continental Shelf, with positions and headings for lost Norwegian vessels. Foreign vessels lost in the same area are not shown.*

An inquiry to all pilot offices in Norway has now indicated several local areas where probabilities for occurrences of extreme waves are believed to be higher than the average, under certain weather conditions. It is now remarkable that such 'Red Areas' agree very well with the mapping of earlier accidents, shown in Fig. 1. Altogether 19 local 'Red Areas' are now identified. (DAHLE, 1979.)

2. BASIC DEFINITIONS

A well defined quantitative description of transient highly asymmetric waves of finite amplitude approaching the point of breaking is needed. In general, finite amplitude storm waves at sea will not appear with a symmetric shape (as a high order Stokes wave), but will have a pronounced asymmetry, both with respect to a vertical and a horizontal axis. This is due to a sheltering effect, which gives rise

to pressure differentials over the upwind and leeward side of the crests. Further, the common wave steepness defined as s = H/L, where H is the total wave height and L is the wave length, does not represent a unique definition of steepness for extreme waves, as several asymmetric waves can exist with the same total steepness s, buth with very different steepnesses of the wave crests.

The present study utilises the advantages that are contained in a zero-downcross analysis. This analysis uses the wave trough and the proceeding wave crest in the definition of a single wave, and defines the wave height as the difference between these water levels, Fig. 2. (The conventional zero-upcross analysis defines a single wave as a wave crest and the following wave trough, and *thus obtains a wave height behind and not ahead of a possible breaking wave.)* The zero-downcross analysis is therefore believed to be the only analysis which provides parameters that are a representation of the physical conditions with relevance to breaking waves, and thus, the only parameters which should be correlated with measurements of ship response or shock pressures.

Furthermore, careful observations show that the wave trough ahead of a breaking wave always appears with a certain and very characteristic shape, and finally the zero-downcross wave height is the only height corresponding to visual wave observations. It is thus only oceanographic wave data treated with the zero-downcross analysis that represents a reasonable basis for a comparison with the vast amount of existing wave observations, made from observers on ships and shore, collected and distributed by national meteorological institutions.

The present study provides a more accurate description of steepness and asymmetry in transient near breaking waves, when the three following parameters are introduced:

Crest front steepness:

$$\varepsilon \equiv \frac{\eta'}{L'}$$

Vertical asymmetry factor:

$$\lambda \equiv \frac{L''}{L'}$$

Horizontal asymmetry factor:

$$\mu \equiv \frac{\eta'}{H} \qquad (1)$$

The definitions are shown in Fig. 2. Here η' is the crest elevation measured from mean water level, while L' and L" are horizontal distances defining the position of the wave crest relative to the zero-crossing points. It is generally accepted that use of the crest elevation for design applications provides a basic parameter more relevant to finite amplitude wave geometry than the wave height. Observations of breaking waves show that these waves can be characterized by a very steep crest front and high asymmetry factors. The ε-parameter is thus a mean front crest inclination.

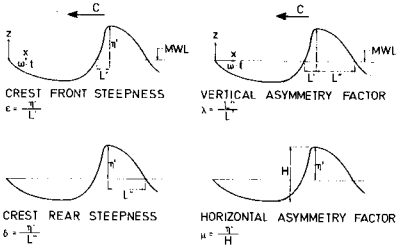

Fig. 2. *Basic definitions for asymmetric waves of finite height. (KJELDSEN & MYRHAUG, 1978.)*

In this study the mean water level, MWL is defined as the still water level in a wave flume before the start of an experiment. For field data the mean water level is defined as the arithmetric mean of a 20 minutes recording period of surface fluctuations.

Thus, in our definition λ describes asymmetry with respect to the vertical axis in the crest, while μ describes asymmetry with respect to a horizontal axis in the mean water level. It is now possible to obtain the crest rear steepness directly as: $\delta \equiv \varepsilon/\lambda = \eta'/L''$.

In the following deterministic experiments in the laboratory with extreme deep water waves will be described in section 4. A range of variation and maximum values of the parameters ε, μ and λ will be given, both for the case with interacting deep water waves, and for the case with interacting waves superposed upon an opposing shear current.

Then, in section 5 results from a statistical analysis of 25000 storm waves from Norwegian waters are given. This

analysis provides joint probability density distributions that relate the ε-parameter to a particular sea state. Thus, a tool from which estimates for probabilities for occurrences of steep and breaking waves in deep water might be obtained.

3. EXPERIMENTAL ARRANGEMENT

A new transient test technique is developed for generation of extreme storm waves in deep water. The waves appear as plunging breakers, deep water bores and spilling breakers, together with very steep near breaking waves, and are created from wave-wave interactions of several individual single wave components.

In deterministic laboratory experiments extreme waves are obtained at a specified time and location. At the Norwegian Hydrodynamic Laboratories this new technique is now developed to a level where on-line testing of fixed and floating structures under extreme deterministic conditions is possible and already undertaken. However, in this study only test series with extreme waves freely dispersing without interaction with structures will be discussed. The test arrangement is shown in Fig. 3.

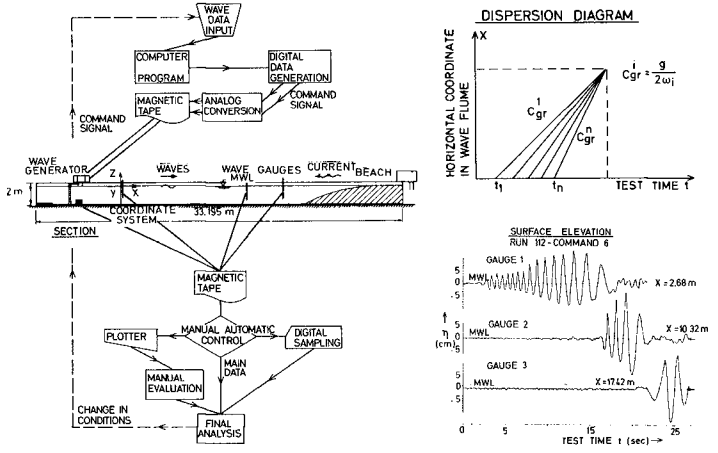

Fig. 3. *Arrangement for wave-wave and current-wave interaction experiments.*

Comprehensive series of experiments were performed in a 33 m long, 1 m wide and 1.60 m deep wave flume, equipped with a computer controlled hinged flap type wave generator at one end, and an energy absorbing parabolic beach at the other end. Further, it was possible to introduce a surface current at the beach with a discharge of 0.050 m^3/sec. The current opposes the dispersion direction of the waves and is extracted in front of the wave generator. The extreme breaking waves in deep water were obtained using several methods. One of them was to utilize the dispersion properties of gravity waves in a wave train. When the rate of change of the cyclic frequency for the wave train was kept constant, a transient event was obtained, where all available wave energy was concentrated at one nodal point in the flume, 12 m from the wave generator, Fig. 3. Surface elevations were measured with wave staffs, and fluctuating particle velocities with electromagnetic current meters.

Synoptic recordings of the surface form and breaker development were obtained with a high-speed movie camera operated with 300 frames/sec. synchronously with the wave staffs. The obtained synoptic wave profiles were then digitized with great accuracy in a motion analyzer.

In a model basin there are major difficulties in obtaining accurate measurements of breaking waves, or of the response of structures to breakers. One is that of generating highly non-linear finite amplitude water waves without scale effects in the flume (without correspondence to the ocean). Such sources of inaccuracy are:

1) Generation of higher harmonics which propagate with phase velocities other than the basic wave. Superposition of such harmonics on the basic wave gives rise to disturbances in the breaking process itself.
2) The wave-induced mass transport is not reproduced correctly in a wave flume. In the ocean, non-linear waves give rise to a drift velocity in the direction of propagation. In a wave flume this net drift is reflected by the beach and returns to the wave generator, and thus a circulation pattern is obtained, with the result that the kinematic profiles in the waves have no mean drift and therefore are not similar to the kinematic profiles in the ocean.

The new transient test technique avoids some of these difficulties, and takes advantage of the small time domain in which progressing waves occur with the correct drift velocity, before unwanted harmonic transients from the wave generator reach the section of observation.

4. EXPERIMENTAL RESULTS

A striking result of the experiments with breaking waves in deep water, is that the observed wave-wave interaction phenomena lead to the generation of breaking waves which can all be classified as (belonging to) three distinct types of wave forms, Fig. 4. It is obvious that many different forms of breaking waves can exist in deep water during advanced sea states. However, when only two-dimensional waves are considered, the number of wave forms decreases rapidly.

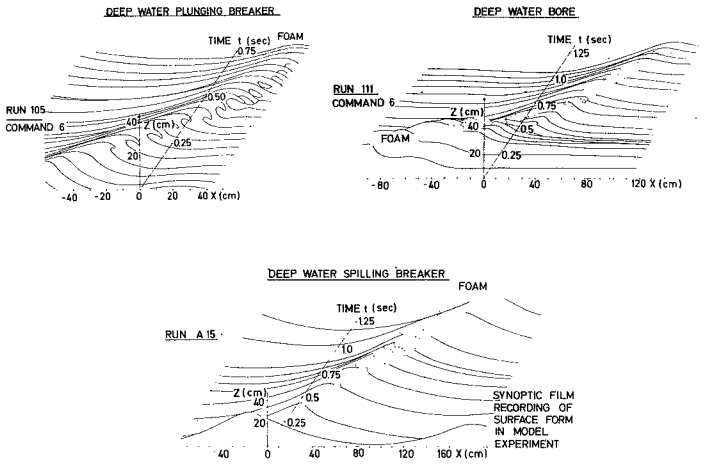

Fig. 4. *Classification of breaking waves in deep water.*

The first type is a deep water plunging breaker, which is a violently breaking wave, generated by interaction of several individual waves. The second type is a deep water bore. This breaker appears as a result of a highly non-linear wave-wave interaction phenomenon, in which one wave phase overtakes another. The overlying wave proceeds in a way which can be observed to be very similar to the travel of a tidal bore. The duration of the breaking is much longer than for a normal spilling breaker, and the asymmetry is very pronounced, with crest elevations which can approach 90% of the total wave heights. When the two wave phases finally meet, the whole front is nearly vertical and breaking.

The third breaker type, observed as results of wave-wave interaction experiments, is the spilling breaker, commonly known as "white capping". This breaker is a very symmetrical breaking wave. This study reports experimental evidence of all three. It is therefore a contribution to the classification of types of breaking waves in deep water, akin to the work by GALVIN (1968), in which breaking waves on beaches were classified.

Particular attention should be given to the results concerning the particle velocities in breaking waves. Fig. 5 gives a map of the horizontal velocity component at five levels for a situation with a plunging breaker, generated from a highly non-linear interaction of several waves in a wave train. In these experiments the rate of change of cyclic frequency was kept constant. The map is obtained as the mean of 26 plunging breakers, which all broke at the same nodal point under identical test conditions. Standard deviations for the measured surface elevations are plotted on the surface contour in order to demonstrate the accuracy of the experiments. The current meter was installed beneath the point where the wave profile became vertical, and the map gives the development in time of the particle velocity and the surface elevation at this position. The linear phase velocity c_{oB} corresponds to the measured wave period at the point of breaking. A considerable phase lag is found between the wave crest and the point where the maximum in the horizontal particle velocity appears. This effect is partly due to limitations in the dynamic response of the current meters. In deep water plunging breakers approximately one wave amplitude below mean water level, the measured particle velocities showed only minor deviations from linear theory.

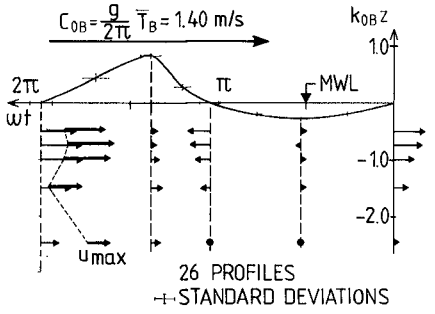

Fig. 5 *Non-dimensional plot of surface elevation and horizontal particle velocities in plunging breakers as functions of time*

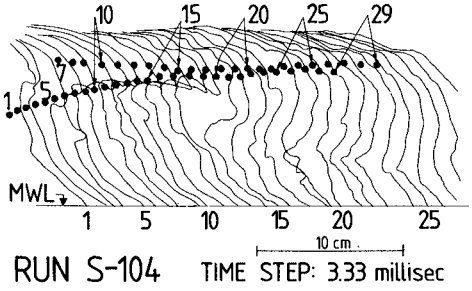

Fig. 6 *Particle trajectories in the crest of a plunging breaker*

Fig. 6 gives an example of the particle trajectories for a Stokes wave disturbed by a subharmonic with equal amplitude. Results are obtained from a high-speed film (300 frames/sec) with neutrally buoyant styropor particles as tracers. The map shows subsequent particle positions in the wave crest near the breaking zone. Particle velocities up to 3.76 m/sec, corresponding to 2.8 times phase velocity c_{OB} for a wave period T_B = 0.85 sec at the point of breaking, were recorded.

In a numerical model (VINJE & BREVIG, 1980), the development of the (breaking) wave profile, the particle velocities and the accelerations within the wave are simulated. The results are achieved up to the point where the overhanging crest hits the wave front. Comparison of the plunging breakers generated in the wave flume and calculated numerically, shows good agreement with respect to

the wave geometry. The measured and calculated velocities also agree well at depths larger than approximately one wave amplitude below the mean water level. In the wave crest near the plunging jet, the measured velocities are, however, 1.5 times as large as the calculated velocities. This may be due to the difference in the method of generating the plunging breakers in the two cases (KJELDSEN, VINJE, MYRHAUG, BREVIG, 1980).

It is a common observation at sea, that steep waves have a tendency to break, sometimes as plunging breakers when they disperse into an area with an opposing surface shear current with a vertical velocity gradient. However, experiments with this particular phenomenon have never been attempted. Therefore, in the following, particular attention will be given to two experiments; one is a case with wave-wave interactions which create a deep water plunging breaker in still water. The other experiment is performed with the same deterministic command signal to the wave generator, but now the wave-wave interaction takes place on a weak steady shear current, which opposes the dispersion direction of the waves. Fig. 7 shows the profile of the current as it was obtained from a film recording, using styropor particles as tracers.

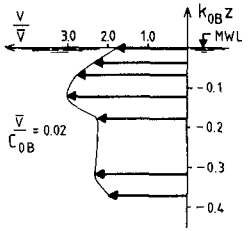

Fig. 7. *Current profile before start of transient wave experiment. Total depth is* $K_{0B} \cdot z = 7.02$. *Mean current velocity is* $\bar{v} = 0.03$ *m/sec.*

Fig. 8 shows the time developments of two deep water plunging breakers. T_B is the period of the breaking waves obtained from wave staffs at the position of breaking. Relative time $t/T_B = 0$ indicates the moment when the wave front becomes vertical. To the left is shown the development with no shear current present. A small jet develops and plunges down in the front of the wave at

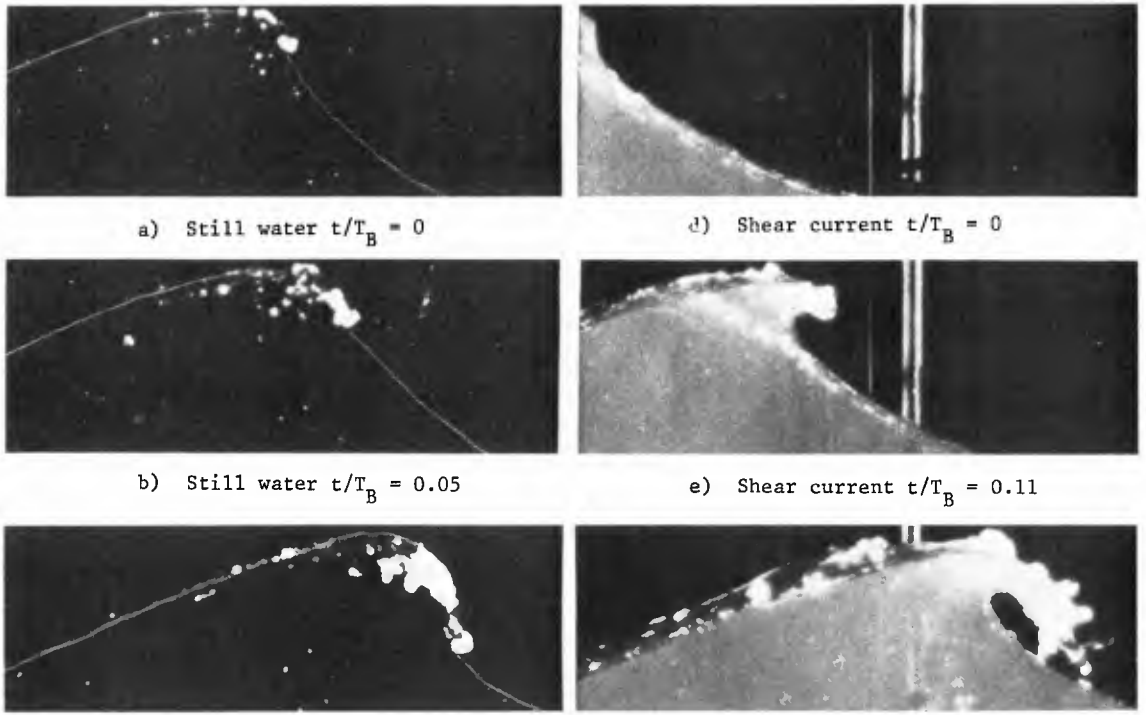

Fig. 8. *Comparison of developments of deep water plunging breakers in still water and in water with an opposing shear current.*

time 0.05. At time 0.11 air has been entrained and development of the breaking on the front increases. Here a large eddie that curls down on the front face of the wave appears, and more and more air is entrained.

To the right is shown the development when a steady shear current is present. The mean current velocity is only 2% of the linear phase velocity computed for the breaking wave. However, the result is remarkable. A much more violent plunging breaker with a very strong jet in the wave crest appears. It shoots forward with a very characteristic shape at time 0.11 and hits the front of the breaking wave at time 0.22. Thus, the duration of the breaking is much longer, and displays the breaking of a much more violent wave.

Fig. 9 shows the development of the two breakers displayed by the ε parameter. Data is obtained from a frame to frame analysis of the film with time steps 10 millisec. At the time the wave fronts become vertical both breakers have ε values near 0.70. For the case with the shear current ε increases during the breaking to a value near 0.83, returning to values near 0.70. For the breaker development in still water, on the other hand, 0.73 is the maximum value, and ε then decreases when breaking takes place.

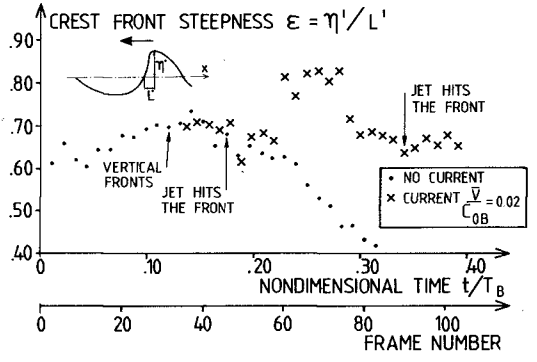

Fig. 9. *Amplification of crest front steepness by a shear current.*

Also the μ-parameter displays the development in a similar way, Fig. 10. When the wave fronts become vertical, both breakers show ratios of crest elevation to the wave heights as high as 0.75-0.80. For the case with a shear current the values of the μ-parameter then increases to nearly 0.90. For the case with no current, the μ-value slowly decreases when the breaker develops.

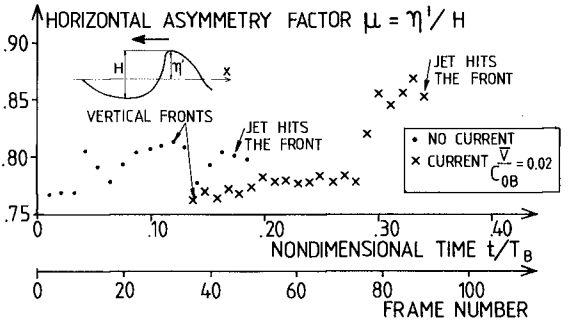

Fig. 10. *Amplification of horizontal asymmetry factor by a shear current.*

The amplification on the plunging breaker can be described as the relative increase in the ε and μ parameters:

$$\Delta\varepsilon = \frac{\varepsilon'^{\text{current}}_{\max} - \varepsilon_{\max}}{\varepsilon_{\max}} = \underline{13\%} \qquad \Delta\mu = \frac{\mu'^{\text{current}}_{\max} - \mu_{\max}}{\mu_{\max}} = \underline{6\%} \qquad (2)$$

Here $\varepsilon_{\max}$ is the maximum value for a wave-wave interaction experiment, while $\varepsilon'^{\text{current}}_{\max}$ is the maximum value for a wave-wave interaction experiment with a shear current superimposed. Similar symbols are used for the μ-parameter. It is striking that a weak current (only 2% of the phase velocity) is able to create such drastic changes in the wave dynamics. The steepening of linear waves in the same shear current is very modest. This means that when a very asymmetric highly non-linear wave is triggered by even a weak energy flux, remarkable non-linear effects can be obtained.

Neither analytical nor numerical models are yet able to describe the phenomenon observed here. Such a high degree of amplification of breakers might lead to serious problems for mariners in smaller vessels in cases where high and steep waves approach even a weak current with a modest gradient. The phenomenon observed in deep water is a parallel to the well-known development of a plunging breaker on a beach, where return flow from the preceding wave can be observed to trigger the development of the following wave, in such a way that it might break as a plunging breaker. (KJELDSEN & OLSEN, 1968.)

5. RESULTS FROM FIELD DATA

Storm Model

No single mathematical model for extreme wave statistics has gained universal acceptance. NOLTE (1973) used storm models which contained the most probable maximum wave height during a storm as a stochastic parameter. ARHAN et al. (1979) used a similar model based on significant wave height. MO, VIK & HOUMB (1978) used a model where consecutive values of $H_{1/3}$ exceed a threshold level, under the condition that also a higher level later is exceeded within a given time.

In the present study a storm model is given by the probability distribution:

$$S(H^*) = \sum_{i=1}^{N} \theta\,(H_{1/3}^{i} - H^*)/N \qquad (3)$$

where the Heaviside unit function is defined by:

$$\theta(x-\xi)_i = \begin{cases} 1 \text{ for } x \geqslant \xi \\ 0 \text{ for } x < \xi \end{cases} \qquad (4)$$

Here $H_{1/3}$ is the significant wave height for the i^{th} storm, N is the total number of storms and H^* is a wave height threshold level. This threshold level is taken as a definition of 'a gale' for the model. In this study only sea state 6, 7, 8 and 9 will be of importance, and a gale will therefore be defined as an event where the significant wave height exceeds 4 m.

With the assumption that storms are statistical independent events, no grouping correction is required. In this way the present model is superior to other methods. Only waves with zero-downcross wave heights exceeding 5 m were found to be significant for evaluation of stability and safety (from capsizing) for the vessels under consideration in the project "SHIPS IN ROUGH SEAS". From available field measurements on the Norwegian continental shelf, nearly 25000 single storm waves with heights exceeding 5 m were analyzed statistically. (KJELDSEN & MYRHAUG, 1978.) Approximately 8% of the most severe sea states in 26 gales were then selected for a closer study, and joint probability density distributions as well as marginal density distributions for relevant parameters were obtained. (KJELDSEN & MYRHAUG, 1979a.) The field data were sampled in the period 1974-78 with 3 wave rider buoys, located at Tromsøflaket, Halten and Utsira, Fig. 1. 20 minutes of recording was obtained every 3 hours, starting 20 minutes before 0 time GMT. The properties of the obtained probability density distributions show that data obtained from the 3 locations can be regarded as belonging to the same statistical population. This means that common statistical distributions can be obtained, which are representative for the wave dynamics in the whole area. (KJELDSEN & MYRHAUG, 1979b.) R.m.s.-values are used for normalisation, and dimensionless plots of probability density distributions are then obtained. The resulting data base provides a coupling to sea state, wind velocity and wave spectral parameters.

Probability density distributions of crest front steepness and asymmetry factors for waves with $H > 5$ m

Fig. 11 shows the probability density distributions of the crest front steepness ε, the vertical asymmetry factor λ, and the horizontal asymmetry factor μ, respectively, for 1754 storm waves with wave heights exceeding 5 m. For all distributions correlation coefficients are obtained using the Pearson χ^2-test.

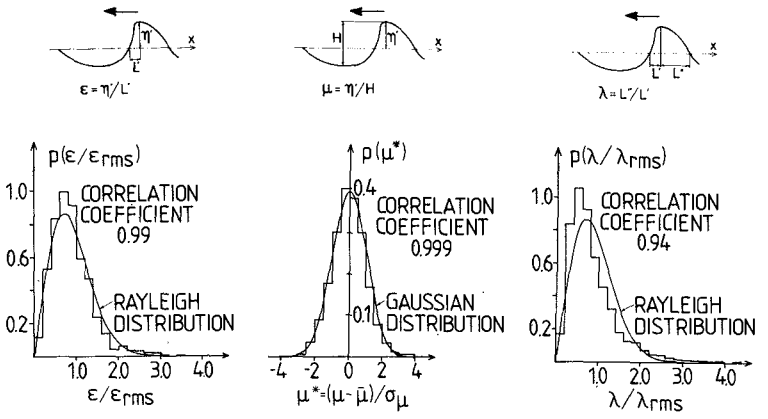

Fig. 11. *Probability density distributions for* ε, μ *and* λ.

The histogram of the crest front steepness ε is compared with the Rayleigh distribution:

$$p(x) = 2x \cdot \exp(-x^2) \qquad (5)$$

where in this case $x = \varepsilon/\varepsilon_{rms}$ is the normalized crest front steepness. ε_{rms} is calculated for wave heights exceeding 5 m. A good correlation with a correlation coefficient of 0.99 is obtained. A two-parameter Weibull distribution is also fitted to the histogram of the crest front steepness. According to the two-parameter Weibull distribution, the cumulative probability is given by:

$$P(x \leqslant x_c) = 1 - \exp(-(\frac{x_c}{B})^{\gamma}) \qquad (6)$$

where x_c is a specific value. The result is given in Table 1. (The Rayleigh distribution corresponds to $\gamma = 2$ and $B = 1$.) The distribution of the vertical asymmetry factor λ also shows a good correlation with the Rayleigh distribution with a correlation coefficient of 0.94. The Weibull parameters are given in Table 1. The horizontal asymmetry factor shows a very good correlation with the Gaussian distribution given by

TABLE 1. WEIBULL PARAMETERS FOR MARGINAL DISTRIBUTIONS

	Normalized wave height h/ξ			Normalized crest front steepness $\varepsilon/\varepsilon_{rms}$			Normalized total wave steepness s/s_{rms}			Normalized wave period t/ζ			Normalized vert. asymmetry factor λ/λ_{rms}		
	γ	B	Corr. coef.	γ	B	Corr. coef.	γ	B	Corr. coef.	γ	B	Corr. coef.	γ	B	Corr. coef.
$H \geq 5$ m				1.67	.91	.997							1.44	.86	.99
All waves	2.02	.94	.998	1.45	.83	.998	1.85	1.00	.99	3.67	.93	.997			

Two-parameter Weibull distribution $P(x \leq x_c) = 1 - \exp\left(-\left(\frac{x_c}{B}\right)^{\gamma}\right)$

TABLE 2. WEIBULL PARAMETERS FOR CONDITIONAL DISTRIBUTIONS

Normalized wave height h/ξ	Normalized crest front steepness $\varepsilon/\varepsilon_{rms}$			Normalized total wave steepness s/s_{rms}			Normalized wave period t/ζ		
	γ	B	Correlation coefficient	γ	B	Correlation coefficient	γ	B	Correlation coefficient
0 -0.2	1.55	1.10	.98	2.96	1.52	.92	3.11	.51	.89
0.2-0.4	1.70	1.08	.99	1.80	1.17	.996	3.61	.67	.96
0.4-0.6	1.39	.84	.997	1.77	.99	.99	3.81	.80	.99
0.6-0.8	1.33	.73	.995	1.66	.91	.98	4.43	.97	.97
0.8-1.0	1.43	.68	.99	1.87	.85	.99	5.12	1.10	.92
1.0-1.2	1.50	.76	.997	1.98	.92	.99	5.09	1.20	.93
1.2-1.4	1.71	.90	.99	3.25	1.22	.93	5.30	1.25	.90
1.4-1.6	1.89	.95	.996	2.37	1.09	.99	5.35	1.35	.87
1.6-1.8	2.22	1.24	.99	4.25	1.50	.94	5.41	1.22	.90
1.8-2.0	3.22	1.38	.95	3.61	1.44	.98	5.54	1.29	.87
2.0-2.2	3.24	1.37	.94	3.52	1.41	.97	5.55	1.39	.83
2.2-2.4	5.17	1.99	.91	4.80	1.78	.93	5.65	1.33	.83
2.4-2.6	5.32	1.70	.88	5.62	1.90	.87	5.51	1.63	.76

$$p(\mu^*) = \frac{1}{\sqrt{2\pi}} \cdot \exp(-\tfrac{1}{2}\,\mu^{*2}) \qquad (7)$$

where $\mu^* = (\mu-\bar{\mu})/\sigma_\mu$. Here $\bar{\mu}$ is the mean value of μ and σ_μ^2 is the variance of μ in the respective registration period calculated for wave heights exceeding 5 m. A correlation coefficient of 0.999 was obtained.

Joint probability density distribution of crest front steepness and wave height

Fig. 12 shows the joint probability density distribution of crest front steepness and wave height combined for all three locations, representing 6353 storm waves.

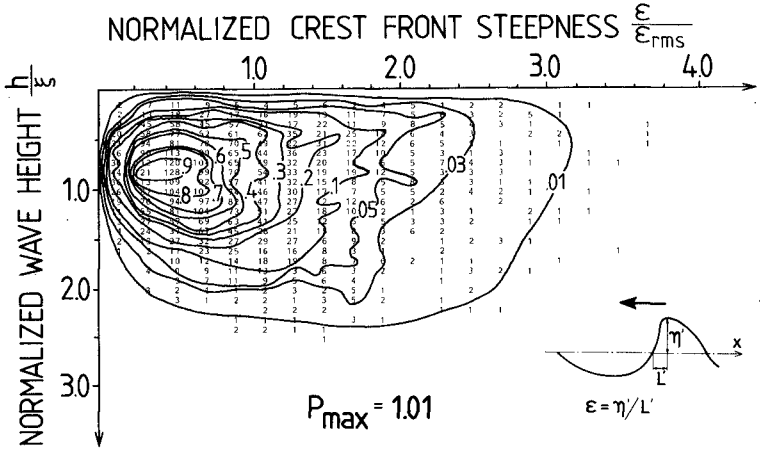

Fig. 12. *Joint probability density distribution of ε and H.*

The marginal distributions of the wave height and the crest front steepness are given in Fig. 15, showing good correlations to the Rayleigh distribution. Correlation coefficients of 0.98 were obtained for both distributions. Weibull parameters and correlation coefficients for the marginal distributions are included in Table 1. Further, the Weibull distribution given in (6), was fitted to the conditional distribution of the crest front steepness.

Weibull parameters and correlation coefficients corresponding to the best fit for each wave height interval are given in Table 2. If the crest front steepness and the wave height were uncorrelated, then the conditional distribution of the crest front steepness for given wave heights would be a Rayleigh distribution. However, the degree of correlation between ε and H is given in Table 2.

Joint probability density distribution of total wave steepness and wave height

Fig. 13 shows the joint probability density distribution of total wave steepness and wave height combined for all three locations. The marginal distribution of total wave steepness is given in Fig. 15, and corresponds well to the Rayleigh distribution with a correlation coefficient of 0.92. Weibull parameters are given in Table 1. The Weibull parameters for the conditional distribution of the total wave steepness for each wave height interval are given in Table 2. A marginal distribution of s that follows the Rayleigh distribution is in agreement with earlier results (BATTJES, 1976), but in our study use of the rms-value is recommended for normalisation. The s-H distribution shows a similar general shape as the ε-H distribution, and is included here in order to obtain a comparison of different types of steep waves.

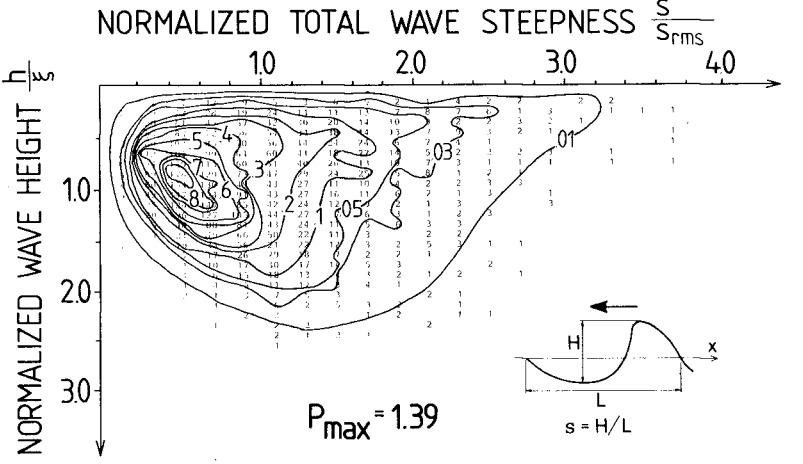

Fig. 13. *Joint probability density distribution of s and H.*

Joint probability density distribution of wave height and wave period

Fig. 14 shows the joint probability density distribution of wave height and wave period combined for all three locations. The wave period was normalized with the parameter $\zeta^2 = (\overline{T^4})^{1/2}$, related to the rms-value of the wave period squared. The marginal distribution of the wave period is given in Fig. 15. The histogram is compared with the Rayleigh distribution of the wave period squared, i.e.

$$p(\frac{t}{\zeta}) = 4(\frac{t}{\zeta})3 \cdot \exp(-(\frac{t}{\zeta})^4) \qquad (8)$$

and shows a good correlation with a correlation coefficient of 0.98. Weibull parameters are given in Table 1. (The distribution of the wave period in (8) corresponds to $\gamma = 4$ and $B = 1$. The Weibull distribution is also fitted to the conditional distribution of the wave period for each wave height interval, Table 2. The joint probability density distribution of wave height and wave period shows asymmetry with respect to wave periods for lower waves and symmetry for higher waves, having the same general behaviour as the joint distribution given by CAVANIÉ et al. (1976).

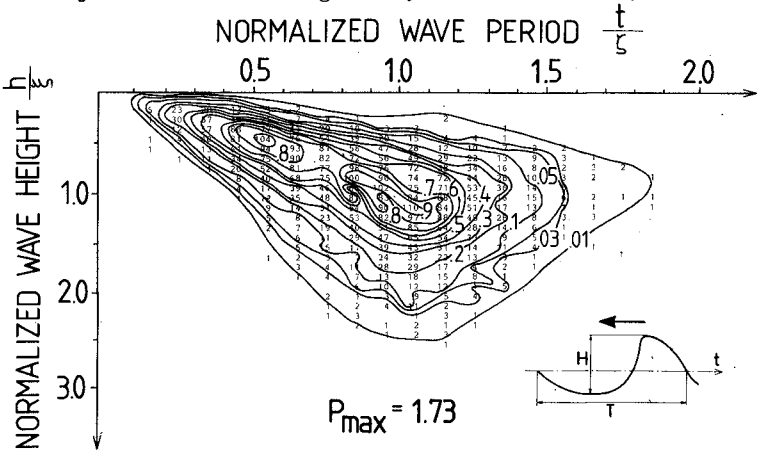

Fig. 14. *Joint probability density distribution of H and T.*

Assuming a narrow band spectrum, LONGUET-HIGGINS (1975) found a theoretical joint distribution of H and T with an axis of symmetry at the mean period of the spectrum. This describes the observed joint distribution for high waves. A detailed comparison of LONGUET-HIGGINS and CAVANIÉ et al.'s theory is given by GODA (1978).

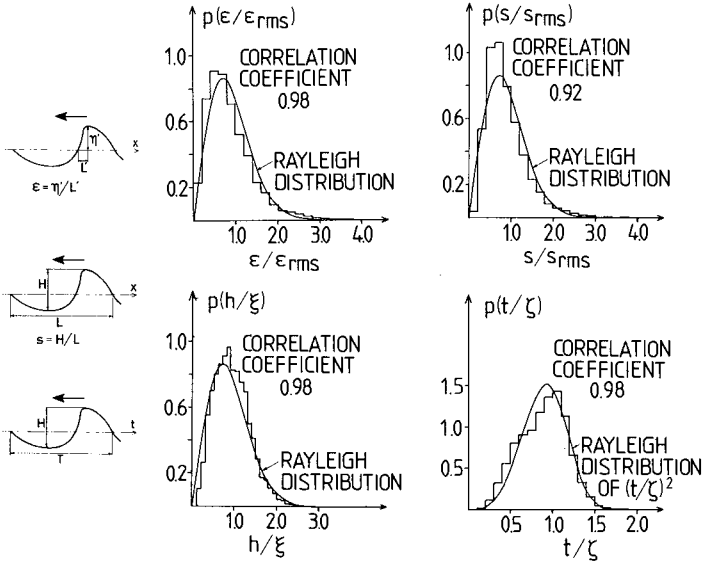

Fig. 15. *Marginal distributions of ε, s, H and T.*

6. DISCUSSION OF RESULTS

An analysis of 6353 storm waves showed that asymmetric waves with heights H > 5 m and vertical asymmetry factor $\lambda > .2$ appeared more frequently in wave groups than asymmetric waves with H > 5 m and horizontal asymmetry factor $\mu > 0.67$. (KJELDSEN & MYRHAUG, 1979a.)

Fig. 11 shows that the horizontal asymmetry factor follows a Gaussian distribution for H > 5 m. An application of this result is that for waves with a given specific wave height (h), 16% of these waves will have crest heights that exceed:

$$\eta' = (\bar{\mu} + \sigma_{\mu})h \tag{9}$$

while 2.5% of the waves with the specific wave height, h, will have crest heights that exceed:

$$\eta' = (\bar{\mu} + 2\sigma_{\mu})h \tag{10}$$

This result has obvious important applications for the evaluation of both safety and design.

A very rough sea state can only be satisfactorily described as an event that contains both high values for the wave heights and high values for steepness and asymmetry parameters. High values of steepnesses combined with low values of wave heights describe a choppy sea, but this is not disastrous. Low values of steepnesses combined with high values of wave heights describe a heavy swell. *It is therefore the joint probability density distributions for high values of both steepnesses and wave heights that describe a very rough sea, and not the percentage of breaking waves itself.* Thus, the term *extreme waves* used earlier, describes a condition with high values of both wave height and crest front steepness.

When estimates of probabilities of occurrences of breaking waves are made, then the joint distribution of wave height and wave period is commonly used. A breaking criteria is then formulated in terms of the total wave steepness s. However, the parameter s does not define a steep asymmetric wave uniquely. Several asymmetric waves can exist, with the same total wave steepness s, but with very different crest front steepnesses, see Fig. 16.

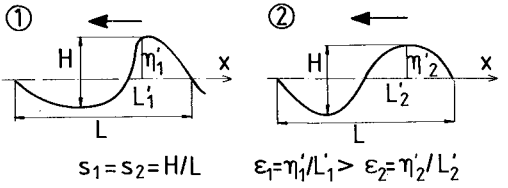

Fig. 16. *The total wave steepness s does not define an asymmetric wave uniquely.*

Thus, the joint probability density distributions of s and H or of H and T are not suited, when estimates for probabilities for occurrences of breaking waves are made.

This study has shown that the crest front steepness is the most relevant parameter describing the mean inclination of the wave profile ahead of the crest, while the zero-downcross wave height is obtained ahead of a breaking wave. Therefore, when estimating probabilities for occurrences of breaking waves, the use of the joint distribution of crest front steepness and zero-downcross wave height is recommended.

7. CONCLUSIONS

1) The experiments show that all two-dimensional breaking waves generated by wave-wave or current-wave interactions in deep water can be classified as belonging to one of three distinct types, namely deep water plunging breakers, deep water bores, and deep water spilling breakers.

2) The difference in phases between a basic wave and a disturbance is crucial for the creation of a deep water plunging breaker.

3) A weak opposing shear current with a mean velocity of only 2% of the linear phase velocity for the breaking wave, was able to amplify a deep water plunging breaker violently. Thus, the relative increase in the μ-parameter became 6%, while the relative increase in the ε-parameter became 13%.

4) Recommendations for analyzing of steep asymmetric waves are to use:

   - zero-downcross analysis defining the wave height as the height ahead of the wave crest, giving a parameter relevant for the description of the development of the breaking process, and for the response of ships and structures.

   - the crest front steepness ε, the vertical asymmetry factor λ and the horizontal asymmetry factor μ in order to describe the zero-downcross wave uniquely.

5) Field data from the Norwegian Sea shows that the probability density distributions of the crest front steepness ε, and the vertical asymmetry factor λ follows the Rayleigh distribution. The horizontal asymmetry factor μ follows the Gaussian distribution. It was found that for waves with wave heights beyond 5 m, a high vertical asymmetry factor λ was obtained more frequently than a high horizontal asymmetry factor μ. Maximum values obtained in the field data and the laboratory experiments were $\lambda = 7.7$, $\varepsilon = 0.83$ and $\mu = 0.92$. A high μ-value indicates that the crest height is very near the total wave height. *In other words, the wave is nearly entirely above mean water level.* This latter result is obviously important both for evaluations of safety and design.

6) Joint probability density distributions of the following zero-downcross wave parameters are given:

- *Crest front steepness and wave height*
- *Total wave steepness and wave height*
- *Wave height and wave period*

Conditional distributions for given wave heights are presented as two parameter Weibull distributions. The joint distribution of H and T shows asymmetry with respect to wave periods for lower waves, and symmetry for higher waves, in the same general pattern as the one given by CAVANIÉ et al. (1976). Since s does not define steep asymmetric waves uniquely, neither the joint distribution of s and H nor the joint distribution of H and T should be used to estimate probabilities of occurrences of breaking waves.

7) Severeness of a particular sea state, containing estimates for the probabilities of occurrences of breaking waves, should be evaluated from the given joint probability density distribution of crest front steepnesses and wave heights *for individual zero-downcross waves.* This method will be superior to a method using mean parameters such as a mean wave period and a significant wave height.

8. ACKNOWLEDGEMENTS

Experiments with current-wave interactions were performed as a part of the project "Shock Pressures from Breaking Waves" sponsored by the Royal Norwegian Council for Scientific and Industrial Research (NTNF).

Other experiments and analysis of field data were performed as a part of the project "Ships in Rough Seas" sponsored by the Royal Norwegian Council for Scientific and Industrial Research (NTNF), the Norwegian Maritime Directorate and the Norwegian Fisheries Research Council (NFFR).

9. REFERENCES

ARHAN, M.F., CAVANIÉ, A.G., EZRATY, R.S., 1979: "Determination of the Period Range associated to the Design Wave". Paper No. 3643. Proc. Offshore Technology Conf., Houston, Texas.

BATTJES, J.A., 1976: "Probabilistic Aspects of Ocean Waves". International Research Seminar on Safety of Structures under Dynamic Loading, Trondheim 1977, Vol. 1, pp. 387-439.

CAVANIÉ, A., ARHAN, M. & EZRATY, R., 1976: "A Statistical Relationship between Individual Heights and Periods of Storm Waves". Proceedings BOSS '76, Vol. II, pp. 354-360.

DAHLE, L.A., 1979: "Waves and Weather Conditions on the Norwegian Continental Shelf - Mapping of Dangerous Areas", Report, Ships in Rough Seas, Part 4, Norwegian Hydrodynamic Laboratories, Trondheim, Norway (in Norwegian).

GALVIN, C.J., 1968: "Breaker Type Classification on Three Laboratory Beaches", Journal of Geophysical Research, Vol. 73, No. 12, June.

GODA, Y., 1978: "The Observed Joint Distribution of Periods and Heights of Sea Waves". Proc. 16th Conference on Coastal Engineering, Hamburg, Vol. I, pp. 227-246.

KJELDSEN, S.P., VINJE, T., MYRHAUG, D., BREVIG, P., 1980: "Kinematics of Deep Water Breaking Waves", Paper No. 3714, Proc. 12th Offshore Technology Conf., Houson, Texas.

KJELDSEN, S.P., MYRHAUG, D., 1979a: "Formation of Wave Groups and Distributions of Parameters for Wave Asymmetry", Report No. STF60 A79044. Ships in Rough Seas, Part 4. Norwegian Hydrodynamic Laboratories, Trondheim, Norway.

KJELDSEN, S.P., MYRHAUG, D., 1979b: "Wave-Wave and Wave-Current Interactions in Deep Water", Proc. 5th POAC Conference, Trondheim, Vol. III, pp. 179-200.

KJELDSEN, S.P., MYRHAUG, D., 1978: "Kinematics and Dynamics of Breaking Waves", Report No. STF60 A78100, Ships in Rough Seas, Part 4. Norwegian Hydrodynamic Laboratories, Trondheim, Norway.

KJELDSEN, S.P., OLSEN, G.B., 1968: "Breaking Waves" (16 mm film). Institute of Hydrodynamics and Hydraulic Engineering (ISVA), Technical University of Denmark, Copenhagen.

LONGUET-HIGGINS, M.S., 1975: "On the Joint Distribution of the Periods and Amplitudes of Sea Waves". Journal of Geophysical Research, Vol. 80, No. 18, pp. 2688-2694.

LONGUET-HIGGINS, M.S., 1969: "A Non-Linear Mechanism for the Generation of Sea Waves". Proc. Roy. Soc. A, 311: 371-389.

MO, K., VIK, I., HOUMB, O.G., 1978: "Wave Statistics at Station "M" with Special Reference to Duration and Frequency of Sea States". Division of Port & Ocean Engineering at The University of Trondheim, Norway.

NEDRELID, T., 1978: "Analysis of Earlier Capsizing Accidents", Report, Ships in Rough Seas, Part 3, Norwegian Hydrodynamic Laboratories, Trondheim, Norway (in Norwegian).

NOLTE, K.G., 1973: "Statistical Methods for Determining Extreme Sea States". Proc. 2nd POAC Conf., Reykjavik, Iceland.

VINJE, T., BREVIG, P., 1980: "Numerical Simulation of Breaking Waves", 3rd Int. Conference on Finite Elements in Water Resources, Univ. of Mississippi, USA.

10. NOMENCLATURE

c_{oB}	linear phase velocity at point of breaking $\left(\frac{g}{2\pi}T_B\right)$	$V(zK_{oB})$	current velocity at level zK_{oB}
H	zero-downcross wave height	$\bar{V}$	mean current velocity
h	specific zero-downcross wave height	x	horizontal coordinate
K_{oB}	wave number at point of breaking $\left(\frac{4\pi^2}{gT_B^2}\right)$	z	vertical coordinate, origo at MWL
L	zero-downcross wave length	δ	crest rear steepness ($= \eta''/L''$)
L'	forward length from zero-upcross point to crest	ε	crest front steepness ($= \eta'/L'$)
L''	backward length from crest to zero-downcross point	ζ	parameter related to rms-value of squared wave period ($\zeta^2 = \sqrt{\frac{m_0}{m_4}}$)
s	total zero-downcross wave steepness	η'	crest elevation
T	zero-downcross wave period	λ	vertical asymmetry factor ($= L''/L'$)
T_B	zero-downcross wave period at point of breaking	μ	horizontal asymmetry factor ($= \eta'/H$)
t	time coordinate	μ^*	($= (\mu-\bar{\mu})/c_\mu$) normalisation of μ
$\bar{t}$	specific zero-downcross wave period	$\bar{\mu}$	mean value of μ
u	horizontal particle velocity in breaking wave	ξ	root-mean-square of the zero-downcross wave height
		c_μ	standard deviation of μ